Journal of Operation and Automation in Power Engineering
Vol. 10, No. 3, Dec. 2022, Pages: 179-188
http://joape.uma.ac.ir

A New Fuzzy Direct Power Control of Doubly-Fed Induction Generator in a Wind Power System

A. Hasanzadeh[1], *H. Shayeghi*[1, 2], *S. R. Mousavi-Aghdam*[*, 1]

[1]*Department of Electrical Engineering, University of Mohaghegh Ardabili, Ardabil, Iran*
[2]*Energy Management Research Center, University of Mohaghegh Ardabili, Ardabil, Iran.*

Abstract- *This paper presents a new fuzzy direct power control of double-fed induction generators (DFIG) in the wind power system. The most important issue in the application of DFIG generators is proper control of the active and reactive powers of these generators, which are generally carried out by vector control or direct torque/power control methods. Direct power control (DPC) directly controls the active and reactive powers of the stator, and stems from results from direct torque control. To use the vector control method, it is necessary to use conventional PI controllers the main disadvantage being the controller robustness due to the nonlinear behavior of the wind turbine and blade oscillations, and it is unavoidable that after a while, the controller's coefficients need to be updated. Therefore, the main purpose of this paper is to present a direct power control method based on fuzzy construction to overcome the mentioned problem. Simulation results of the proposed strategy are extracted under different performance conditions, and these results are compared with the conventional vector-oriented control method. These comprehensive results exhibit the effectiveness of the proposed fuzzy DPC method for the DFIGs based wind power systems.*

Keyword: Direct power control, double-fed induction generator, fuzzy control, wind power system.

1. INTRODUCTION

In recent decades, the use of renewable energy systems has been the focus of many researchers. The penetration of clean and unlimited renewable energy sources, especially wind and solar sources, is daily increasing due to the depletion of fossil fuel resources, the increase in the price of these sources, and their environmental pollution problems. Generally, using wind energy as an endless energy source, the world's current electricity capacity could be doubled. The purpose of operating wind power plants is to reduce the costs associated with generating energy and to decrease the environmental pollution. The doubly-fed induction generator (DFIG) is a widely used generator in variable-speed wind turbines. DFIG is in fact the induction generator whose stator is directly connected to the electrical grid and whose rotor is connected to the grid via a back-to-back electronic power converter. The DC voltage control of DC-link and active and reactive power control of DFIG are the duty of the grid side converter and the rotor side converter of the back-to-back converter in DFIG, respectively. It is observed that the active and reactive power control operates independently by applying vector control (VC) strategy to the rotor side converter in the direction of the stator flux [5]. In this method, PI controllers have been used to implement the vector control of the doubly-fed induction generator, however, the main disadvantage of the PI controller is that it is the resistant to partial system parameters. In Ref. [6], a neural grid controller is proposed for this purpose, one of its disadvantages being the need to separate d-q components of the rotor current. The direct power control (DPC) method has a faster response and higher accuracy than VC, and the steady-state response of the DPC is better in comparison to the VC [7-9]. However, it is perceived that the wind turbine system due to the nonlinear behavior and also due to some fluctuations that may disrupt the system will not have the same response on the contrary of linear controllers [10-11]. Therefore, it will be necessary to adjust the control coefficients repeatedly.

Comparison of the vector control method with the direct power control method is verified in literature [12-13]. The DPC exhibits better performance than other methods in this regard. To separate the active power from the reactive power control, the oriented flux vector control of the stator with the rotor position sensor has been used. In this method, a sensor is required to detect

Received: 28 Aug. 2020
Revised: 04 Nov. 2020, 09 Jun., 05 Jul., and 19 Jul. 2021
Accepted: 23 Aug. 2021
∗Corresponding author: (Seyed Reza Mousavi-Aghdam)
E-mail: r.mousaviaghdam@uma.ac.ir
DOI: 10.22098/joape.2022.7662.1545
Research Paper

the position of the rotor to control the active and reactive powers, while the DPC does not need such a sensor. A variable-speed and constant-frequency wind energy conversion system using DFIG are intended in Ref. [14] to design and compare two separate control strategies for the RSC and the GSC. The results show that the relative convergence of the system's dynamic response to the reference values. In general, the DPC method based on two hysteresis controllers is a more appropriate method for connecting the wind turbine to the grid. In Ref. [15] three types of DPC strategies for DFIG based wind power generation system have been proposed including DPC rotor flux method (RF-DPC), DPC stator flux method (SF-DPC), and Predictive direct power control method (P-DPC). A DPC method is presented in Ref. [16], in which the RSC is acted according to the proper selection of the voltage vector based on the difference between the reference value and the measured value of active and reactive power and the position of the rotor flux. The performance of the control method during faults is also important. In Ref. [17] the performance of DFIG-based wind turbine is studied by the VC method during short circuit. Moreover, in Ref. [18] a combination of the VC method and direct power control for the RSC is considered. The results show that the proposed method in Ref. [18] has the advantages of vector control and direct power control in a compact control system and exhibits more reliability. Ref. [19], suggested a self-sensing technique for flux-oriented control (FOC), which is used in different load conditions with different principles. Vector control in the stator flux reference frame can help to control the output power and voltage of the disconnected DC line [20]. In Ref. [21] a new method for direct control of DFIG power is proposed with dual supply using slip mode controller. To implement this method, it is not necessary to separate the components of the rotor current.

Modulation techniques are also considered in the control of DFIGs. In Ref. [22] a new DPC strategy is offered for DFIG-based wind power systems using discrete space vector modulation (DSVM). Using different modulations techniques may cause some disadvantages. To increase the efficiency of the closed-loop system, the fuzzy system may be used. In Ref. [23] a DPC for a DFIG-based wind system is presented with a new method that rotates the segment space in a clockwise or counterclockwise direction to improve the efficiency of the switching table. In such a system, the fuzzy control method can be implemented. The mentioned method reduces the active and reactive power ripples and THD of the injected current at different speeds. This method is robust to changes in machine parameters, but a real test must be used for the accuracy of the proposed method. In order to conversion of wind energy and regulation of DFIG in Ref. [24] a new approach of direct power control (DPC) of DFIG based model predictive direct power control is developed. The optimal switching vector state of two-level voltage source inverter (2L-VSI) is extracted by minimizing two cost functions to select the voltage vectors for stator active and reactive power in synchronously manner. The proposed method is verified by the simulation results compared to the DPC and PPC methods [24]. In Ref. [25], the model predictive control (MPC) method is proposed to control the power converter employed in the rotor side of DFIG. This method along with the use of an incremental algorithm applies a sequence of weighting factors in the cost function over the prediction horizon to predict a longer horizon with relatively low computational burden and maximize the impact of primary samples on the optimal vector selection. In Ref. [26], the DPC method based on the nonlinear backstepping controller associated with the Lyapunov function was designed to control the stator powers and help the operation of the DFIG generator during the faults and ensure the stability and robustness of this system. in this technique the reactive power was injected into the network to contribute to the return of voltage, and set the active power to the optimum value to suppress the high peak currents. In order to verify the performance and effectiveness of the DPC-BS method, the proposed technique is compared with the classical vector control (VC) using Proportional-Integral (PI) correctors. In Ref. [27], an efficient Direct Power Control (DPC) method based on an experimental implementation study of the Wind Energy Conversion System (WECS) is proposed for stand-alone mode operation of variable wind speed DFIG. Also, the L, LC and LCL passive filters are implemented between the DFIG's rotor circuit and the inverter to improve the power quality. Some of the main advantages of the proposed control system are the simple control and Implementation, fast dynamic response, and good power quality injected to RL-load.

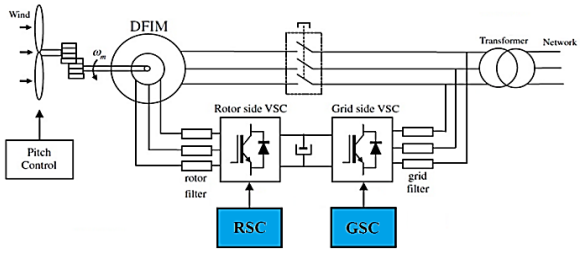

Fig.1. Configuration of DFIM power system with back-to-back converter

In this paper, a new control scheme using the modified fuzzy DPC method is proposed for DFIG-based wind system control. First, the description and mathematical modeling of the DFIG system are presented in section 2. In Section 3, the DPC method for the DFIG is given along with the main control principles. In section 4, the proposed fuzzy system is designed for the DPC and the method implementation will be explained. Finally, in section 5, the simulation results will be provided and discussed considering three different scenarios. The effectiveness of the proposed fuzzy DPC method is verified by simulation results.

2. DESCRIPTION OF DFID-BASED POWER SYSTEM

2.1. Wind power system configuration

A simplified diagram of a DFIM-based wind power system is shown in Fig.1, which shows how the studied back-to-back converter is connected to the grid by the grid-side filter as well as the rotor-side filter from DFIM.

The wind power which is obtained from the wind turbine will be transmitted to the grid through the back-to-back converter. Switching pulses from the controller are generated considering a two levels voltage source. By adjusting the DC link voltage from the obtained voltages, the reactive power is exchanged with the grid. This is usually done in closed-loop control. The method used for this controller is often the VC method which is based on the orientation of the d axis to the space vector of the grid voltage. By passing the active power through the rotor, it must cut off the DC link and then transmit it to the grid. Therefore, by adjusting the DC link voltage, this controller also indirectly affects the exchange of active power with the grid. The actual value of the DC link voltage is first subtracted from its reference value and passed through a PI controller to obtain the amount of active grid power nonlinearly. Finally, by converting two obtained references for the voltage components and using one of the modulation methods, SPWM is used in this paper, the necessary pulses are provided for GSC.

2.2. Modelling of the DFIG

According to the model of AC machines developed by several researchers, the DFIM model can be summarized and ideally can be described by using three windings on the stator side and three windings on the rotor side. These windings are an ideal representation of a real machine that can be used to obtain an equivalent electrical circuit. Under this model, the voltages, currents, and instantaneous fluxes of the machine can be described by the following electrical equations:

$$v_{as}(t) = R_s i_{as}(t) + \frac{d\psi_{as}(t)}{dt} \quad (1)$$

$$v_{bs}(t) = R_s i_{bs}(t) + \frac{d\psi_{bs}(t)}{dt} \quad (2)$$

$$v_{cs}(t) = R_s i_{cs}(t) + \frac{d\psi_{cs}(t)}{dt} \quad (3)$$

where, R_s is the stator resistance, $i_{as}(t)$, $i_{bs}(t)$ and $i_{cs}(t)$ are the stator phase currents. $v_{as}(t)$, $v_{bs}(t)$ and $v_{cs}(t)$ are the stator voltages and $\psi_{as}(t)$, $\psi_{bs}(t)$ and $\psi_{cs}(t)$ are the stator flux linkages, respectively. The electrical angular frequency on the stator side, ω_s, is imposed by the grid. The rotor side equations are similarly defined as follows:

$$v_{ar}(t) = R_r i_{ar}(t) + \frac{d\psi_{ar}(t)}{dt} \quad (4)$$

$$v_{br}(t) = R_r i_{br}(t) + \frac{d\psi_{br}(t)}{dt} \quad (5)$$

$$v_{cr}(t) = R_r i_{cr}(t) + \frac{d\psi_{cr}(t)}{dt} \quad (6)$$

where R_r is the resistance of the rotor winding and $i_r(t)$, $i_{br}(t)$ and $i_{cr}(t)$ are the rotor currents. $v_{ar}(t)$, $v_{br}(t)$ and $v_{cr}(t)$ are the rotor voltages and $\psi_{ar}(t)$, $\psi_{br}(t)$ and $\psi_{cr}(t)$ are the rotor flux linkages. All rotor parameters and variables are referred to the stator. The relationship between the angular frequency of the stator and the rotor can be represented as follows:

$$\omega_r + \omega_m = \omega_s \quad , \quad \omega_m = p\Omega_m \quad (7)$$

where, ω_m is the electrical angular frequency of the rotating shaft, and p is the number of pole pairs. The changes of this parameter will make the equations nonlinear. Therefore, the equations are transferred to an appropriate reference frame as the following. Using the space vector transformations in the stator reference frame, the corresponding equations will be obtained. The space vector formulation of the mentioned equation can be represented as follows:

$$\vec{V}_s^{\,s} = R_s \vec{i}_s^{\,s} + \frac{d\vec{\psi}_s^{\,s}}{dt} \quad (8)$$

$$\vec{V}_r^{\,r} = R_r \vec{i}_r^{\,r} + \frac{d\vec{\psi}_r^{\,r}}{dt} \quad (9)$$

where $\vec{V}_s^{\,s}$ is the voltage space vector of stator, $\vec{i}_s^{\,s}$ is the current space vector of stator and $\vec{\psi}_s^{\,s}$ is the space

flux linkages vector of stator. The same notations are used for the rotor parameters explaining subscripts of *s* and *r* represent the space vectors referred to the stator and rotor parameters and superscripts referred to the stator and rotor frames. The relation between flux linkages and currents can be written as:

$$\vec{\psi}_s^{\,s} = L_s \vec{i}_s^{\,s} + L_m \vec{i}_r^{\,s} \tag{10}$$

$$\vec{\psi}_r^{\,r} = L_m \vec{i}_s^{\,r} + L_r \vec{i}_r^{\,r} \tag{11}$$

where L_s is the stator inductance, L_r is the rotor inductance, L_m is magnetization inductance, $L_{\sigma s}$ is leakage inductance of the stator and $L_{\sigma r}$ is the leakage inductance of rotor, that can be represented as follows:

$$L_s = L_{\sigma s} + L_m \tag{12}$$

$$L_r = L_{\sigma r} + L_m \tag{13}$$

Now, by referring to the same frame, the equations can be represented as follows:

$$\vec{V}_s^{\,s} = R_s \vec{i}_s^{\,s} + \frac{d\vec{\psi}_s^{\,s}}{dt} \tag{14}$$

$$\vec{V}_r^{\,s} = R_s \vec{i}_r^{\,s} + \frac{d\vec{\psi}_r^{\,s}}{dt} - j\omega_m \vec{\psi}_r^{\,s} \tag{15}$$

$$\vec{\psi}_s^{\,s} = L_s \vec{i}_s^{\,s} + L_m \vec{i}_r^{\,s} \tag{16}$$

$$\vec{\psi}_r^{\,s} = L_m \vec{i}_s^{\,s} + L_r \vec{i}_r^{\,s} \tag{17}$$

The active and reactive electrical powers supplied to the stator and rotor sides can be calculated using the space vectors of the voltages and currents as follows:

$$P_s = \frac{3}{2}\mathrm{Re}\left\{\vec{V}_s.\vec{i}_s^{\,*}\right\} \quad , \quad P_r = \frac{3}{2}\mathrm{Re}\left\{\vec{V}_r.\vec{i}_r^{\,*}\right\} \tag{18}$$

$$Q_s = \frac{3}{2}\mathrm{Im}\left\{\vec{V}_s.\vec{i}_s^{\,*}\right\} \quad , \quad Q_r = \frac{3}{2}\mathrm{Im}\left\{\vec{V}_r.\vec{i}_r^{\,*}\right\} \tag{19}$$

in which the star superscript is a complex conjugate of the space vectors. Finally, the electromagnetic torque can be written as follows:

$$T_{em} = \frac{3}{2}\frac{L_m}{\sigma L_r L_s} p\,\mathrm{Im}\left\{\vec{\psi}_s^{\,*}.\vec{\psi}_s\right\} = \frac{3}{2} L_m p\,\mathrm{Im}\left\{\vec{i}_s.\vec{i}_r^{\,*}\right\} \tag{20}$$

where leakage ratio is $\sigma = 1 - L_m^2 / L_s L_r$ and p is the number of poles pairs in the machine. By rewriting the equations (14)-(17) and selecting the flux linkages as state variables, the DFIM state equations can be represented as follows:

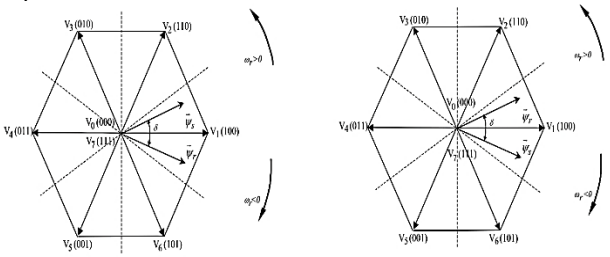

Fig. 2. Space magnetic flux vectors in the (a) motor mode and (b) generator mode [1]

$$\frac{d}{dt}\begin{bmatrix}\vec{\psi}_s^{\,s}\\ \vec{\psi}_r^{\,s}\end{bmatrix} = \begin{bmatrix}\dfrac{-R_s}{\sigma L_s} & \dfrac{R_s L_m}{\sigma L_s L_r}\\ \dfrac{R_r L_m}{\sigma L_s L_r} & \dfrac{-R_r}{\sigma L_r} + j\omega_m\end{bmatrix}.\begin{bmatrix}\vec{\psi}_s^{\,s}\\ \vec{\psi}_r^{\,s}\end{bmatrix} + \begin{bmatrix}\vec{V}_s^{\,s}\\ \vec{V}_r^{\,s}\end{bmatrix} \tag{21}$$

Expanding the equation (21) in terms of $\alpha\beta$ components, the following expression can be obtained:

$$\frac{d}{dt}\begin{bmatrix}\psi_{\alpha s}\\ \psi_{\beta s}\\ \psi_{\alpha r}\\ \psi_{\beta r}\end{bmatrix} = \begin{bmatrix}\dfrac{-R_s}{\sigma L_s} & 0 & \dfrac{R_s L_m}{\sigma L_s L_r} & 0\\ 0 & \dfrac{-R_s}{\sigma L_s} & 0 & \dfrac{R_s L_m}{\sigma L_s L_r}\\ \dfrac{R_r L_m}{\sigma L_s L_r} & 0 & \dfrac{-R_r}{\sigma L_r} & -\omega_m\\ 0 & \dfrac{R_r L_m}{\sigma L_s L_r} & -\omega_m & \dfrac{-R_r}{\sigma L_r}\end{bmatrix}\begin{bmatrix}\psi_{\alpha s}\\ \psi_{\beta s}\\ \psi_{\alpha r}\\ \psi_{\beta r}\end{bmatrix} + \begin{bmatrix}V_{\alpha s}\\ V_{\beta s}\\ V_{\alpha r}\\ V_{\beta r}\end{bmatrix} \tag{22}$$

Depending on the choice of state space variables, different models of state-space can be concluded. In this model, the stator and rotor voltages, as well as load torque, are regarded as inputs and the stator and rotor currents and flux linkages together with electromagnetic torque and speed are regarded as outputs.

3. DIRECT POWER CONTROL OF DFIG

Connecting the DFIG to the grid requires voltage adjustment to synchronize with the grid voltage. As mentioned before, the DPC method is based on direct control of the active and reactive capacities of the DFIG. Fig. 2 shows the switching sectors and associated space vector in sub or hyper-synchronous modes of operation.

It is important to note that due to the connection of the machine from the grid side, the grid voltage is constant in which case the stator voltages will also be constant, while the stator current depends on how the rotor voltage vectors are selected. To clarify this issue, the following statements can be deduced by substituting machine equations:

$$P_s = \frac{3}{2}\frac{L_m}{\sigma L_s L_r}\omega_s \left|\vec{\psi}_s\right|.\left|\vec{\psi}_r\right|\sin\delta \tag{23}$$

$$Q_s = \frac{3}{2}\frac{\omega_s}{\sigma L_s}\left|\vec{\psi}_s\right|\left[\frac{L_m}{L_r}\left|\vec{\psi}_s\right| - \left|\vec{\psi}_r\right|\cos\delta\right] \tag{24}$$

where δ is the angle between the space vectors of the rotor and the stator magnetic fluxes. The voltage drop across the stator resistance is ignored here. It is assumed that the stator voltage is constant in which case there are many constant expressions in the above equations that can be written as follows:

$$P_s = K_1\left|\vec{\psi}_r\right|\sin\delta \tag{25}$$

$$Q_s = K_2\left[K_3 - \left|\vec{\psi}_r\right|\cos\delta\right] \tag{26}$$

Now, according to these equations, it can be understood how by injecting the rotor voltages, the

location of the fluxes can be changed, and in this case, by changing the flux, their effect on the active and reactive powers of the stator is obtained. By checking the expressions of $\left|\vec{\psi}_r\right|\sin\delta$ and $\left|\vec{\psi}_r\right|\cos\delta$, we will be able to modify the active and reactive powers.

The control diagram block of the DPC method is shown in Fig. 3. It calculates the pulse control strategy without any modulation scheme to control the VSC semiconductors at two levels. This control method will select the appropriate voltage vectors to keep the machine under control. The voltage vector of the rotor is selected directly from the P_s and Q_s errors using the hysteresis controllers. For this purpose, it will select the voltage vector required to correct the errors in the controlled variables. The Q_s controller is based on a two-level hysteresis comparator with hysteresis HQ band, while the P_s controller uses a three-level hysteresis comparator with hysteresis HP band. The schematic of these two types of controllers is also presented in Fig. 3 in yellow boxes. According to Table 1, the required voltage vector will be selected. When the output of the controller is set to 1, it means that a positive change is required, and if it is set to -1, a negative change is required. Both controllers (HP and HQ) must be adjusted to small values to improve accuracy in hysteresis bandwidth controller changes. But these have a limit to the values associated with the minimum switching sampling period (h) of the used hardware to run and the minimum state time of the semiconductors. However, an oscillation in the active or reactive stator powers will be unavoidable. If we assume that the control of a higher-level wind turbine produces a reference torque, so DFIG will be controlled by the torque instead of P_s seen here for DPC.

Table 1. Vector selection based on the torque and magnetic flux controller outputs

		uP_s(torque)		
		1	0	-1
uQ_s(flux)	1	$V_{(k-2)}$	V_0, V_7	$V_{(k+2)}$
	-1	$V_{(k-1)}$	V_0, V_7	$V_{(k+1)}$

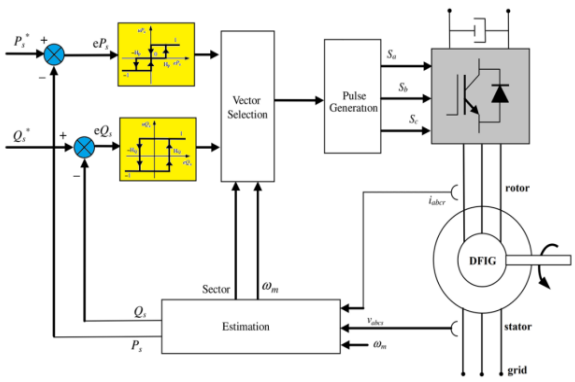

Fig. 3. Diagram block of Direct Power Control (DPC) for DFIG

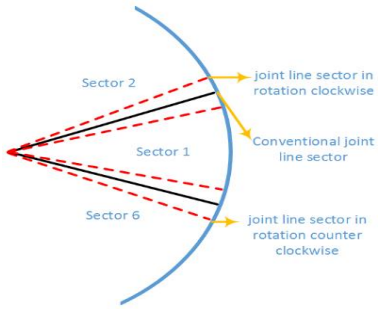

Fig. 4. The new location of the sectors when the stator flux rotates clockwise or counter-clockwise

4. PROPOSED FUZZY BASED DPC STRATEGY

Fuzzy logic gives the control system linguistic flexibility. Soft computing is a computational method that assembles the ability of the human mind distinction for argument in learning an uncertain and inaccurate environment [28]. Suitable for nonlinear systems, it is completely independent of the mathematical equations of the system, which is highly dependent on the personal system. Considering some assumptions, the rotor voltage can be written as follows:

$$\vec{V}_r \simeq \frac{d\vec{\psi}_r}{dt} \tag{27}$$

As it is known, for a two-level three-phase converter, eight switching states can be selected, two of which are zero vectors and the others are space voltage vectors whose amplitudes are the same and the plane is divided into six equal areas. The effect of the voltage vectors of V_2 and V_3, which can change $\left|\vec{\psi}_r\right|\sin\delta$ and $\left|\vec{\psi}_r\right|\cos\delta$, is when the rotor leakage flux is in sector 1 and in clockwise direction. However, the effect of the rotor voltage vector on power changes is the main point that can be considered as a function that depends on the angle between the rotor flux vector and the stator flux vector. Under steady-state conditions, the angular frequencies of the rotor and the stator flux are equal to the synchronous angular frequency, so the space vectors of the flux rotate with the frequency $\omega_m = \omega_s - \omega_r$ in the rotor reference frame. Therefore, it is concluded that the effects of voltage vectors on sub-synchronous and super-synchronous velocities are different.

One way to examine these changes is to propose switching tables for sub-synchronous and super-synchronous speeds. This function will increase the rows of the switch table and it will be very difficult to implement. This will increase the complexity of the system, and when the use of the fuzzy method is considered in the system, it will require more rules and more memory, and as a result, more computation time, which is practically not desirable. In some cases, this

complexity is greater than in switching cases. In addition, another important problem is implementing a switch table. To describe in more detail, it is assumed that the generator rotates at a speed of 1.18 times the synchronous speed. In this case, the stator flux will rotate continuously at 1.18 times the synchronous speed in the rotor reference frame. If DFIG is connected to a 50Hz power grid and the switching frequency is 1 kHz, the location of the stator flux will be $(1.18-1)\times 2\times 50\times \pi/1000$ radians in each switch, which in this example will be 3.24°. It is assumed that this will happen for each switch under the above conditions. Therefore, when it is $\omega_r = 0.82\times\omega_s$ and $\omega_r = 1.18\times\omega_s$, the maximum displacement of the stator flux will be about 6.48°. Therefore, a representation of two switching tables using six vectors and six sectors will be possible. The proposed method in this paper is based on the principle that all sectors will rotate in the opposite direction of the stator flux by about 6.48°. Fig. 4 shows the new position of the sectors. In this way, selecting the vector improves the nearby position of the joint line sectors.

Table 2. Table of switching in DPC method after fuzzification

ΔQ	N	P	N	P	N	P
ΔP	N		Z		P	
M_1	V_2	V_3	V_7	V_0	V_6	V_5
M_2	V_3	V_4	V_0	V_7	V_1	V_6
M_3	V_4	V_5	V_7	V_0	V_2	V_1
M_4	V_5	V_6	V_0	V_7	V_3	V_2
M_5	V_6	V_1	V_7	V_0	V_4	V_3
M_6	V_1	V_2	V_0	V_7	V_5	V_4
M_7	V_2	V_3	V_7	V_0	V_6	V_5

Table 3. The proposed rules of the fuzzy logic controller for ΔP

		$K_D dP_e$				
		NN	***N***	***Z***	***P***	***PP***
$K_E P_e$	***NN***	N	N	N	N	N
	N	N	N	N	N	P
	Z	N	Z	Z	Z	P
	P	N	P	P	P	P
	PP	P	P	P	P	P

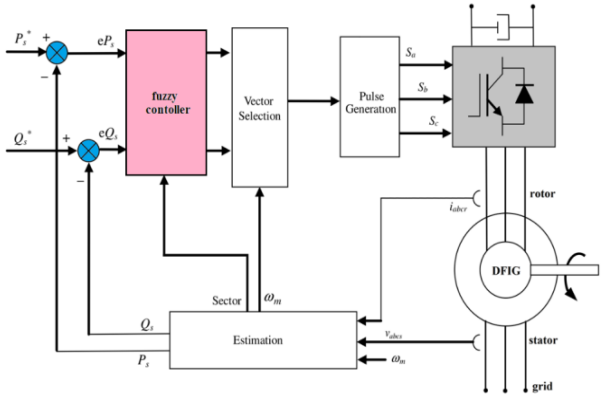

Fig. 5. Schematic diagram of the proposed fuzzy DPC for DFIG

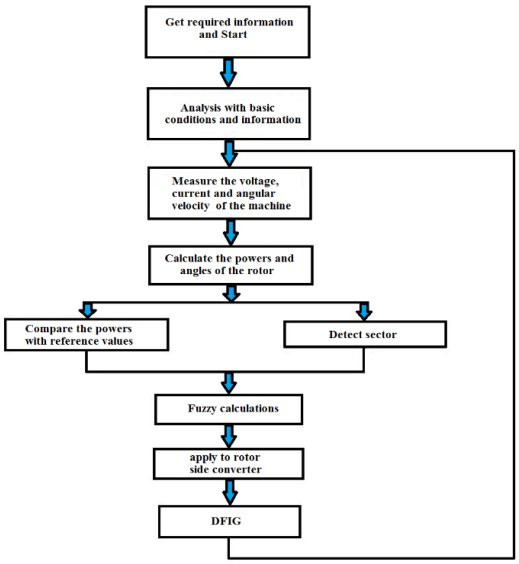

Fig. 6. Proposed fuzzy DPC algorithm flowchart for DFIG

The proposed fuzzy DPC block diagram in the closed-loop model is shown in Fig. 5. The real-time values have resulted from the position of the angular difference between the stator and rotor fluxes and the active and reactive power errors as inputs for the fuzzy system. The rules of the DPC switching are based on Table 2. The new fuzzy rule system for DPC to calculate $_{\Delta P}$ is shown in Table 3. K_E and K_D represent the proportional and derivative coefficients of the active power controller. The flowchart of the proposed strategy fuzzy DPC method is depicted in Fig. 6 in detail. Initially, the required information will be received from the system and the analysis will be performed according to the initial conditions. By measuring the stator voltages and currents, the active and reactive powers will be estimated. The stator and rotor fluxes and the angle between them are obtained from the stator and rotor currents in the stator reference frame. Based on these powers and comparison with the reference values, the differences between these values are obtained. By normalizing them and also considering sector location, they are sent to the fuzzy controller and after the calculations, the output of the fuzzy controller is finally sent as a pulse command. These commands do not require any modulation scheme to the rotor side converter and will be sent to DFIG.

5. SIMULATION AND DISCUSSION

A typical DFIG is selected for simulation and its parameters are summarized in Table 4. The DFIG in this paper has a rated frequency of 50Hz, rated speed of 1500rpm, rated stator power of 2MW. The stator and rotor are star connected and reference active power of 2MW and reference reactive power of 0Var are considered. The voltage of the DC link is about 1150V.

In order to get insight into the proposed control strategy, the system is examined using both the DPC method and the proposed fuzzy DPC method. To precisely assess the proposed control, the system is simulated under different scenarios.

5.1. First Scenario

In the first scenario, the performance of the systems is examined at the normal start of the wind system. There is no variation in the torque or voltage. In the following, the simulation results obtained from conventional DPC and the proposed fuzzy DPC will be compared and discussed. In this section, the simulation time is 4 seconds and both DPC and the proposed fuzzy DPC controllers are running at the same time. Enlarged images of the obtained results are shown for transient moments in times between 0.5 and 1 seconds and for the steady-state in times between 1.5 and 1.8 seconds.

Table 4. DFIG-based wind system parameters

Parameter	Value	Unit
Effective line-to-line rated voltage of stator (rms)	690	V
Effective rated current of each phase (rms)	1760	A
Rotor / stator conversion ratio	1/3	-
Maximum slip	1/3	-
Number of pole pairs	2	-
Stator resistance	2.6	$m\Omega$
Stator leakage inductance	87	mH
Rotor leakage inductance	87	mH
Magnetization inductance	2.5	mH
Rotor resistance referred to stator	2.9	$m\Omega$
Stator inductance $L_s = L_m + L_{si}$	2.587	mH
Rotor inductance $L_r = L_m + L_{ri}$	2.587	mH
Moment of inertia	127	kg.m^2
DC link capacitor capacity	80	mf
DC link resistance	100	Ω
Grid side filter resistance	2×10^{-4}	Ω
Grid side filter inductance	400×10^{-5}	H
Reference speed	1300	rpm

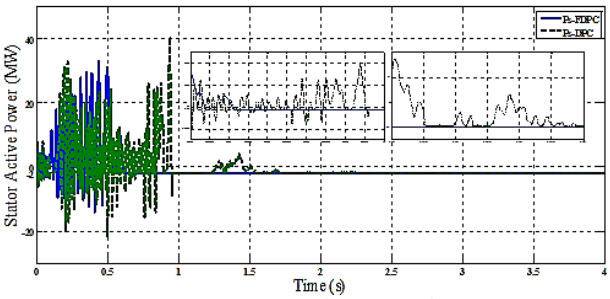

Fig. 7. Active power response of the stator for both control strategies in the first scenario

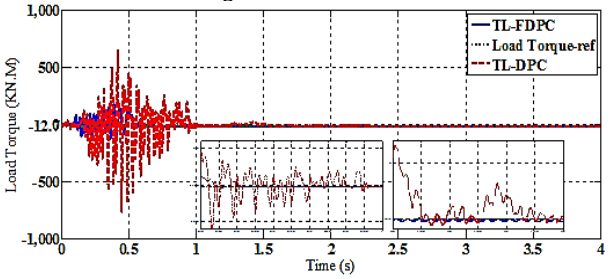

Fig. 8. Load torque response for both control strategies in the first scenario

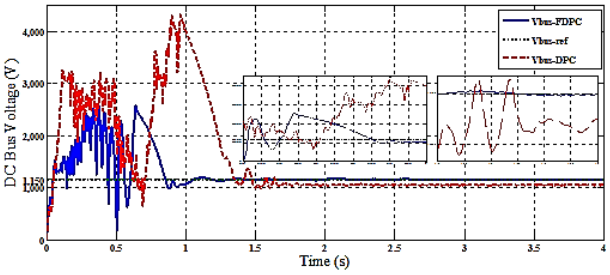

Fig. 9. DC link voltage response for both control strategies in the first scenario

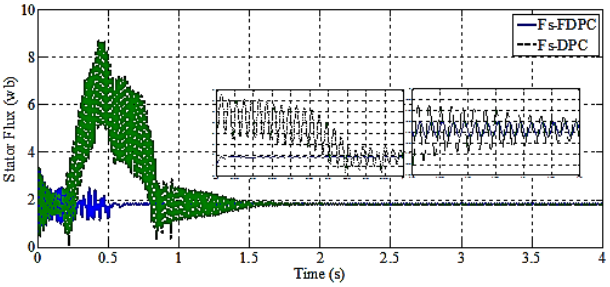

Fig 10. Stator flux response for both control strategies in the first scenario

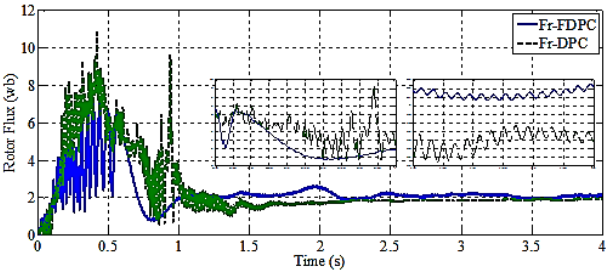

Fig. 11. Rotor flux response for both control strategies in the first scenario

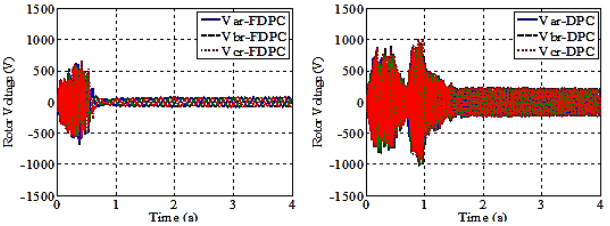

Fig. 12. Three-phase rotor voltage response for both control strategies in the first scenario

The active power of the stator is shown in Fig. 7. In this case, in the proposed DPC mode, it has a faster response than DPC to reach the steady-state. It shows better tracking and after reaching the steady-state, DPC fluctuations are more than the proposed fuzzy DPC. The load torque results are shown in Fig. 8. As shown, the response to reach the constant load torque state of DFIG in generator mode in DPC will be greater than the proposed control. The DC link voltage results are shown in Fig. 9. It is clear that the DFIG steady-state response time for the reference bus voltage of 1150V in the proposed control is faster than the DPC, the overshoot and settling time is shorter in this mode, and the DPC is poorly able to track the reference value.The results of stator and rotor fluxes for both strategies are shown in Fig. 10 and Fig. 11. As shown, the DFIG steady-state

response time for the stator and rotor fluxes in the proposed control is faster than the DPC, and its overshoot and settling time are shorter in this mode, while fluctuations in the DPC are greater. The results of three-phase rotor voltages are shown in Fig. 12. It can be seen from Fig. 13 that the DFIG steady-state response time in the proposed control is faster than DPC. In this case, the overshoot and settling time are less, the frequency of fluctuations in the DPC is higher, and this will cause more stress on the power switches. It should also be mentioned that the amplitude of the rotor voltages is the different because of different running frequencies in the rotor. Therefore, approximately the same magnetic flux should be produced (see Fig. 16).

5.2. Second Scenario

In the second scenario, in order to be able to examine the performance of both control systems while the wind turbine is in circuit, by changing the load and torque, the system must continue to operate properly. The performance of both controllers will be compared at this time. To implement this scenario, we will first run both systems as in the previous case. In the obtained results, the output results between 1.2 to 4 seconds are enlarged. Because of the similarity, some of the figure types presented in the previous section will be skipped. For this purpose, the reference load changes from -2MW to -1MW at 2.5 second in this scenario, and the reference reactive power is 0Var. The results of active power are shown in Fig. 13. As shown, at 2.5 second, as the active reference power changes from -2MW to -1MW, both controllers follow it. However, in the DPC controller, ripple and oscillation are higher. The DC link voltage results are shown in Fig. 14. When the load and torque are changed in the proposed controller, the DC link voltage response with a small peak will remain at the same reference value of 1150V. However, in the DPC controller, which was around 1050V before the changes, it will reach 1150V at the time of the changes, indicating that if the changes in load and torque are large, the controller may reach different values, which leads to instability in the system.

The results of rotor three-phase voltages are illustrated in Fig. 15. It is clear that when the load and torque change, the proposed controller will reach a new value with a jump, but in the DPC controller, it will reach a new value after a period of change. The results of stator and rotor fluxes are illustrated in Fig. 16. It is clear that in the steady-state conditions the rotor flux and stator flux in the proposed method has the proper response rather than the DPC method, and the rotor flux will follow the stator flux with very little difference, but in the DPC controller due to the presence of hysteresis on-off controllers, it causes more differences.

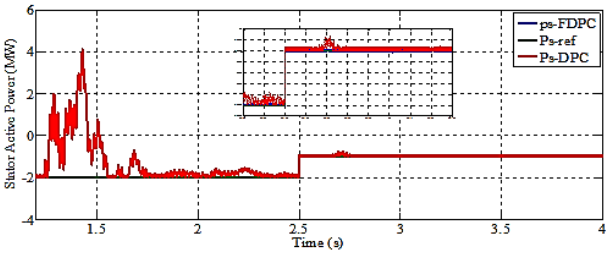

Fig. 13. Active power response for both control strategies in the second scenario

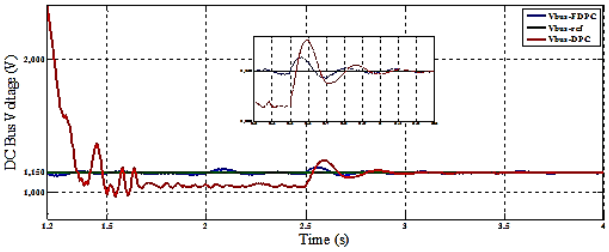

Fig. 14. DC link voltage response for both control strategies in the second scenario

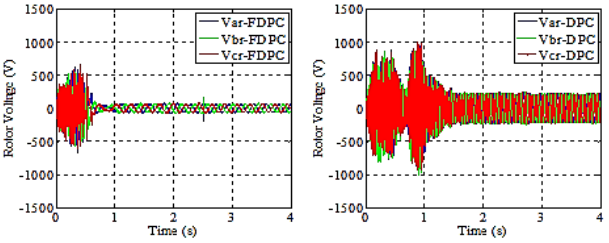

Fig. 15. Three-phase voltage response of rotor for both control strategies in the second scenario

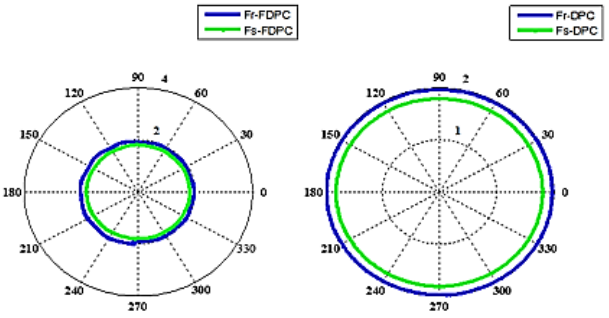

Fig. 16. Response of rotor and stator flux for both control strategies

5.3. Third Scenario

In this subsection, the performance of both control methods is evaluated for a single-phase stator voltage drop of 30% in one of the phases. This abnormal voltage is illustrated in Fig. 17. In the following, the behavior of the system, as well as the performance of both control systems in the face of this voltage drop, will be examined. In this analysis, where the reference active power is -2 MW, the reference reactive power is 0Var, a single-phase voltage drop of 30% in one of the phases is applied in 2.5 second. The results of the active stator power are shown in Fig. 18. It is clear that when applying voltage drop, the system with the proposed controller continues to work with low ripple, but in DPC

controller the intensity of these fluctuations is so high that it may lead to system instability, and in some cases, the system consumes active power from the grid. It means that it has reached the motoring mode.

The results of the three-phase currents of the stator are shown in Fig. 19. When an error occurs in the proposed controller, it continues with a smaller oscillation and shorter response time and with a larger amplitude so that it can fix this error in the system, and in the end, it will still be regular and symmetrical. However, despite less fluctuation at first, the intensity of these fluctuations in the DPC controller is divergent and may carry the system closer to instability.

Table 5. Comparing of two methods considering the ripple of active power (ΔP)

Controlling Method	Ripple of Power (ΔP)
Fuzzy logic controller [23]	0.3685
Fuzzy logic DPC controller	0.2989

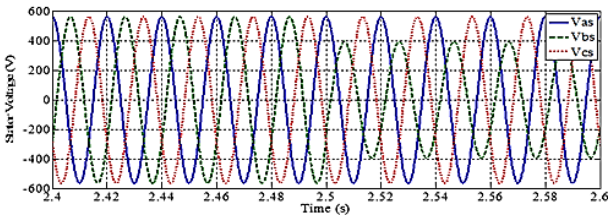

Fig. 17. Single-phase voltage drop of the stator in the third scenario

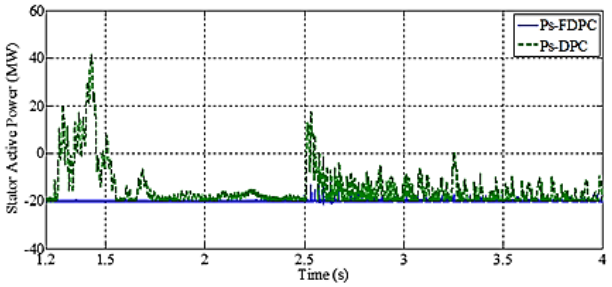

Fig. 18. Active stator power response for both control strategies in the third scenario

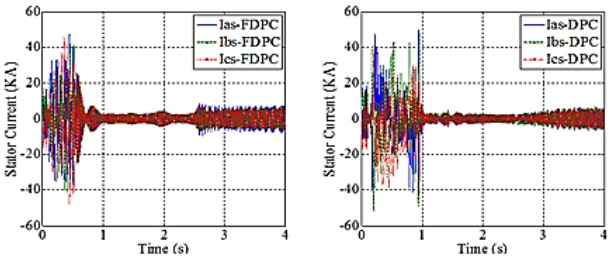

Fig. 19. Three-phase current response of stator for both control strategies in the third scenario

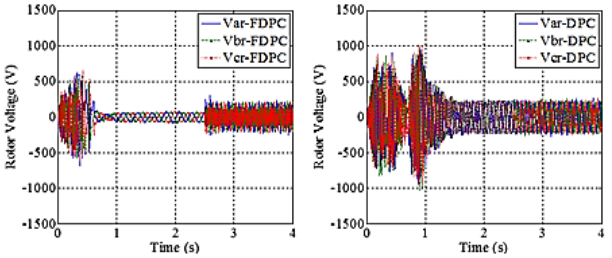

Fig. 20. Rotor three-phase voltage response for both control strategies in the third scenario

The results of the rotor three-phase voltages are also depicted in Fig. 20. It is clear from the figure that when an error occurs in the proposed control, the rotor voltage amplitude is increased to overcome the problem, but the DPC controller only increases the frequency and there are no changes in its amplitude. To performance investigation of the proposed controller, the active power ripple criteria is considered and we define parameter $\Delta P = \int \left| P - P_{ref} \right| dt$ in the definite time period.

The values of this parameter for compression of fuzzy logic controller method and the proposed method are presented in Table. 5. Considering the simulation results, the proposed control strategy presents the proper results in reduced simulation time, simple control algorithm, and also low ripple of active power

6. CONCLUSION

In this paper, a new control scheme is applied to the most common variable-speed wind power system based on DFIG. In general, the system control is divided into two parts including RSC and GSC controls. The strategy of vector-oriented control of the grid side is normally implemented using sinusoidal PWM modulation. However, on the rotor side, there may be more challenges and that is why different control schemes are proposed in this part. The direct control method is the robust and simple method that has been introduced on the rotor side but this control technique has not enough flexibility and in some cases, there must be some adaptive techniques to make it more useful. A suitable fuzzification of direct control of the rotor side without the need for any modulation scheme is an appropriate technique. The use of some fuzzy techniques has very little effect on direct control because of unsuitable design. This paper introduces a new design scheme that has a positive effect on the direct control. The simulation results indicated the suitability the proposed fuzzy direct power control over direct power control in transient and steady states. It mitigates the fluctuations well in most cases and has better dynamic performance in case of faults. It is easier to adjust of the proposed controller and deal with disturbances to keep DFIG in a stable state. The system is verified at three different modes including normal operation, change in load and torque, and application of single-phase voltage dip. The results exhibit the appropriate performance of the proposed system compared with the conventional DPC strategy.

REFERENCES

[1] G. Abad et al., “Doubly fed induction machine modeling and control for wind energy generation applications”,

IEEE Press Series Power Eng., 2011.
[2] F. Blaabjerg, Z. Chen, "Power electronics for modern wind turbines", Morgan & Claypool, 2006.
[3] B. Wu, M. Narimani, "High power converters and ac drives", Wiley IEEE Press, 2017.
[4] M. Kazmierkowski, R. Krishnan, F. Blaabjerg, "Control in power electronics: selected problems", Academic Press Series in Engineering, 2002.
[5] G. Tapia, A. Tapia, J. Ostolaza, "Two alternative modeling approaches for the evaluation of wind farm active and reactive power performance", *IEEE Trans. Energy Conv.*, vol. 21, pp. 909-20, 2006.
[6] O. Soares et al., "Nonlinear control of the doubly fed induction generator in wind power system", *Renew. Energy*, vol. 35, pp. 1662-70, 2010.
[7] H. Nian, P. Cheng, Z. Zhu, "Coordinated direct power control of dfig system without phase-locked loop under unbalanced grid voltage conditions", *IEEE Trans. Power Electron.*, vol. 31, pp. 2905-18, 2016.
[8] D. Sun, X. Wang, "Low-complexity model predictive direct power control for DFIG under both balanced and unbalanced grid conditions", *IEEE Trans. Ind. Electron.*, vol. 63, pp. 5186-96, 2016.
[9] A. Peterson., "Analysis and modeling and control of doubly-fed induction generators for wind turbines", Ph.D. thesis, Chalmers University of Technology, Goteborg, Sweden, 2005.
[10] S. Raju, G. Pillai, "Design and implementation of type-2 fuzzy logic controller for DFIG-based wind energy systems in distribution networks", *IEEE Trans. Sustain. Energy*, vol. 7, pp. 345-53, 2016.
[11] R. Pena, J. Clare, G. Asher, "Doubly fed induction generator using back-to-back PWM converters and its application to variable-speed wind-energy generation", *IEEE Proc. Electr. Power Appl.*, vol. 143, pp. 231-41, 1996.
[12] Y. Rao, A. Laxmi, "Direct torque control of doubly fed induction generator based wind turbine under voltage dips", *Int. J. Adv. Eng. Tech.*, vol. 3, pp. 711-20, 2012.
[13] G. Abad et al., "Direct power control of doubly-fed-induction-generator-based wind turbines under unbalanced grid voltage", *IEEE Trans. Power Electron.*, vol. 25, pp. 442-52, 2010.
[14] J. Alaya, A. Khedher, M. Mimouni, "DTC, DPC and nonlinear vector control strategies applied to the DFIG operated at variable speed", *Wseas Trans. Envir. Develop.*, vol. 6, 2011.
[15] A. Nazari, H. Heydari, "Direct power control topologies for DFIG-based wind plants", *Int. J. Comput. Electr. Eng.*, vol. 4, pp. 475-9, 2012.
[16] A. Boulahia, K. Nabti, H. Benalla, "Direct power control for AC/DC/AC converters in doubly fed induction generators based wind turbine", *Int. J. Electr. Comput. Eng.*, vol. 2, pp. 425-32, 2012.
[17] A. Thin, N. Yuzanakyaing, "Dynamic modelling of doubly fed induction generators based wind turbine system", *Int. J. Ind. Electron. Electr. Eng.*, vol. 3, 2015.
[18] J. Mohammadi et al., "A combined vector and direct power control for DFIG-Based wind turbines", *IEEE Trans. Sustain. Energy*, vol. 5, pp. 767-75, 2014.
[19] G. Marques, M. Iacchetti, "A self-sensing stator-current-based control system of a DFIG connected to a DC-link", *IEEE Trans. Ind. Electron.*, vol. 62, pp. 6140-50, 2015.
[20] Y. Han et al., "A doubly fed induction generator controlled in single-sided grid connection for wind turbines", *IEEE Trans. Energy Conv.*, vol. 28, pp. 413-24, 2013.
[21] S. Roozbehani, K. Abbaszadeh, "A new method for extracting maximum power from a wind turbine system equipped with a doubly-fed induction generator with slip mode control", *J. Energy Eng. Manage.*, vol. 1, pp. 11-22, 2012.
[22] M. Kazemi, M. Moradi, R. Kazemi, "Minimization of powers ripple of direct power controlled DFIG by fuzzy controller and improved discrete space vector modulation", *Electr. Power Syst. Res.*, vol. 89, pp. 23-30, 2012.
[23] M. Kazemi, M. Moradi, R. Kazemi, "Fuzzy logic control to improve the performance of the direct power control based DFIG", *Int. J. Comput. Math. Electr. Electron. Eng.*, vol. 33, pp. 254-72, 2014.
[24] A. Benzouaoui, H. Khouidmi, B. Bessedik, "Parallel model predictive direct power control of DFIG for wind energy conversion", *Int. J. Electr. Power Energy Syst.*, vol. 125, pp. 1-12, 2021.
[25] A. Younesi, S. Tohidi, M. Feyzi, "Computationally efficient long horizon model predictive direct current control of DFIG wind turbines", *J. Oper. Autom. Power Eng.*, vol. 8, pp. 172-81, 2020.
[26] S. Mensou et al., "A direct power control of a DFIG based-WECS during symmetrical voltage dips", *Protection Control Modern Power Syst.*, vol. 5, pp. 1-12, 2020.
[27] F. Amrane, B. Francois, A. Chaiba, "Experimental investigation of efficient and simple wind-turbine based on DFIG-direct power control using LCL-filter for stand-alone mode", *ISA Trans.*, vol. 115, 2021.
[28] M. Moradi, M. Kazemi, E. Ershadi, "Direct adaptive fuzzy control with membership function tuning", *Asian J. Control*, vol. 14, pp. 726-35, 2012.